An experimental survey of the cathodic activation of metals including Mg, Sc, Gd, La, Al, Sn, Pb and Ge in dilute chloride solutions of varying pH

R.L. Liu[1,*], S. Thomas[1], J.R. Scully[2], G. Williams[3], N. Birbilis[1]

[1]Department of Materials Science and Engineering, Monash University, Clayton, VIC 3800, Australia
[2]Department of Materials Science and Engineering, University of Virginia, Charlottesville, VA 22904, USA
[3]Materials Research Centre, College of Engineering, Swansea University, Bay Campus, Crymlyn Burrows, Swansea, SA1 8EN, UK

[*]ruiliang.liu@monash.edu

Abstract:

The kinetics of the hydrogen evolution reaction (HER) have been reported to increase upon pure magnesium (Mg) surfaces, following prior anodic polarisation or corrosion. This phenomenon is termed anodically induced 'cathodic activation', which is not necessarily an elementary concept. The tendencies of other metals to exhibit cathodic activation has not been systematically explored in the past. In this study, an experimental survey of cathodic activation was conducted for different metals on the basis of understanding the origin of the cathodic activation phenomenon on Mg; including the metals Sc, Gd, La, Al, Sn, Pb and Ge, in 0.1 M NaCl with pH ranging from 3-11. Sc, Gd, La and Mg showed cathodic activation in solutions of various pH, whereas Al showed cathodic activation only in an acidic solution. Sn, Pb and Ge did not show significant cathodic activation across the pH range tested. It is proposed on the basis of the results herein, metals that tend to directly react with water to form hydroxides in aqueous electrolytes have a higher tendency to demonstrate cathodic activation.

Keywords: NDE, hydrogen evolution reaction, cathodic activation, magnesium corrosion,

1. Introduction

Magnesium (Mg) dissolution, and indeed Mg corrosion, has been reported to be unique on the basis that as the anodic reaction ($Mg \rightarrow Mg^{2+} + 2e^-$) proceeds, there is an attendant increase in kinetics of the accompanying cathodic reaction[1-6]. In aqueous environments, the cathodic reaction is the hydrogen evolution reaction (HER), given by $2H_2O + 2e^- \rightarrow H_2 + 2OH^-$. This phenomenon has often been termed the 'negative difference effect (NDE)' and whilst having been reported for several decades[1-5, 7-10]. Recently, Williams and co-workers have unambiguously highlighted a so-called anodically induced 'cathodic activation' using the scanning vibrating electrode technique[6]. Cathodic activation is a terminology that specifically ascribes enhanced rates of the HER to ability of the electrode under study to more efficiently support reduction reactions[6]. Cathodic activation is a phenomenon that is detrimental for several functional applications of Mg, for example in primary battery systems, where it will result in parasitic self-discharge of the Mg anode electrode[5, 11, 12]; or simply, self-catalysis of corrosion. The kinetics of the HER increasing upon Mg following anodic polarisation, demonstrating the phenomenon of cathodic activation, has been well presented in aqueous chloride containing solutions[6, 13, 14]. It is also noted that in many cases, simply allowing Mg to corrode in the absence of external polarisation is also sufficient to provide sufficient cathodic activation[15]. In the case of anodic polarisation of Mg, dark filiform-like patterns have been found to gradually evolve upon a dissolving Mg surface, with such regions comprised of a bi-layered film with an outer layer of $Mg(OH)_2$ and inner layer of MgO[13]. There is also evidence to suggest that an increase in surface coverage by this bi-layered film, also increased the rate of HER upon the Mg surface[6, 13, 14, 16, 17].

The physical, atomic level description, of cathodic activation is yet to be unambiguously determined. Indeed, enhanced rates of cathodic activity upon Mg have been – for several decades - attributed to noble metal impurity enrichment upon the Mg surface during anodic polarisation[7, 13, 17-22]. McNulty and Hanawalt[23] proposed that impurity elements such as Fe, Cu, and Ni, which have a low over-potential for the HER and also low solid solubilities in Mg, can increase the Mg dissolution rates when present above certain tolerance limits[23, 24]. The tolerance limit for Fe, Cu and Ni, were 170 ppm, 1000 ppm and 5 ppm respectively[23-25]. It is conceived that these noble impurities when present in Mg, could serve as sites for the cathodic reaction and also could agglomerate upon the Mg surface, during anodic polarisation (from incongruent dissolution favouring Mg dissolution as opposed to dissolution of more noble metals), and thus resulting in their surface enrichment. Such impurity enrichment will

result in an increase in the net surface area of the cathode during anodic polarisation, which can correspondingly increase the rate of HER upon the Mg surface. Such noble metal impurity enrichment upon anodically polarised Mg surfaces, has been detected by several researchers[13, 21, 22]. Taheri et al.[13] visually detected the presence of Fe-rich particles within the bi-layered $Mg(OH)_2$/MgO film formed upon the Mg surface, using transmission electron microscopy. Birbilis et al.[22] found that the Fe concentration increased from 4.1 ppm to 119 ppm, when a charge of 1.2 C/cm^2 was applied to the Mg surface, using nuclear microprobe analysis. Similarly, Cain et al.[21] found that the impurity Fe concentration upon the Mg surface increased by an order of magnitude, after anodic polarisation at -1.625 V_{SCE} for 24 hours, using Rutherford Backscattered Spectroscopy (RBS), but still remained < 1% (1000 ppmw). Most certainly, for Mg-alloys with larger (deliberate) alloy loadings, incongruent dissolution and development of surface alloying element enrichment is readily observed[26-28]. Interestingly, the HER rate has also been found to increase even during the anodic polarisation of high purity Mg (99.98% Mg) and ultra-high purity Mg (containing around 1 ppmw impurity content)[9, 19]. This suggests that cathodic activation, may not solely be due to the surface enrichment of the noble metal impurities alone, and whilst noble metal enrichment is a key factor, it may be one of several physical features that dynamically enhance the HER. Lysne et al.[20] studied the cathodic activation of a range of custom Mg-Fe alloys, with different Fe concentrations ranging from 25 ppmw to 13000 ppmw. A model was developed to estimate the Fe enrichment efficiency after prior anodic polarisation and it was observed that the Fe enrichment efficiency after anodic polarisation is poor (<1%), also implying that noble impurity enrichment alone is not responsible for the cathodic activation seen in Mg – albeit is a key contributor.

During the anodic polarisation of Mg in unbuffered non-chelating electrolytes, a $Mg(OH)_2$/MgO film grows upon the Mg surface [3, 7, 13, 19, 29-31]. This film, in turn, provides the sites for the cathodic HER, as evidenced by scanning vibrating electrode technique measurements of Mg galvanostatically polarised at +1 mA/cm^2 in 0.1 M NaCl[6]. Salleh et al.[32] electrochemically characterised the HER upon $Mg(OH)_2$ coated Mg surfaces, using both global techniques (such as potentiodynamic polarisation) and the local method of scanning electrochemical microscopy (SECM). It was observed that the rate of the HER is around 2 to 3 times faster upon the $Mg(OH)_2$ surface than the pristine Mg surface. In unpublished work, Cain et. al.[33] observed that the cathodic activation of Mg is more prominent in unbuffered aqueous chloride-containing solutions, where the formation of metal hydroxides upon the Mg

surface is favoured. However, in solutions like the Tris (Tris(hydroxymethyl)aminomethane) pH buffer (with pH buffered between 7-8), the cathodic activation is presumably less pronounced since metal hydroxides may not form efficiently upon the metal surface. This indicates that the anodically induced cathodic activation seen in Mg is closely associated with the film growth upon the Mg surface, which was also asserted from the results reported by Rossrucker and co-workers[29].

Cathodic reactions such as the oxygen reduction reaction, ORR ($O_2 + 2H_2O + 4e^- \rightarrow 4OH^-$) have been reported to occur upon the surface oxides/hydroxides of other metals such as zinc and Fe[34-36], however such phenomena has been attributed to the intrinsic semiconducting and doped semiconducting characteristics of the surface film[32, 36]. $Mg(OH)_2$ has poor semiconducting characteristics due to a large band gap (around 7.8 eV)[37] and therefore it may be considered less likely – but in need of further study – that HER is kinetically favoured upon the $Mg(OH)_2$ surface. It is conceded however, that semiconducting properties alone are not the only factor that controls a catalytic surface, and it is also possible that HER takes place as one of the steps for direct reaction between Mg and water. This would suggest that other reactive metals, for example rare-earth metals (including cerium, lanthanum, gadolinium, neodymium, yttrium, etc.) would also show cathodic activation after prior-anodic polarisation, because they also have a tendency to form hydroxides upon their surface by direct reaction with water. However, the phenomenon of cathodic activation upon such metals has never been explored in the past. The invigorated recent research into Mg corrosion has offered insights into the aqueous behaviour of reactive metals, whereby Mg (although stable in most atmospheric conditions) represents a gateway to understanding the electrochemistry of metals not previously studied in aqueous environments. It remains to be determined if the previously reported peculiarities of Mg electrochemistry are actually unique, or whether they in fact are very generic across the reactive metals.

The objective of the work herein is to provide an empirical insight to the anodically induced cathodic activation of a range of metals, specifically including a number of metals that are 'reactive' (with standard reduction potentials < -2 VSHE) and also including metals that are 'hydroxide film formers'. The elements studied were Mg, Sc, Gd, La, Al, Sn, Pb and Ge. The elements were tested using a customised electrochemical cycling test previously reported by Birbilis et al.14, and carried out in 0.1 M NaCl for three different pH conditions (pH 3, 6 and 11), in order to investigate the cathodic activation over a range of conditions where the molecular identity of expected surface films will differ.

2. Experimental procedures

Pure metals of nominally 99.9% purity consisting of Sc, Gd, La, Mg, Al, Sn, Pb, and Ge, were sourced from either Amac alloys (Australia) or Alfa-Aesar (USA). The reactive metals including Sc, La and Gd were stored in mineral oil, whereas the other metals were stored in a dry desiccator. Prior to any testing, metals were cleaned, and ground to a 1200 grit surface finish (using SiC paper), followed by ultrasonic cleaning in ethanol. An electrochemical flat cell (Princeton Applied Research, USA) was used for all electrochemical testing here, employing a conventional three-electrode configuration with a Pt-mesh counter electrode and a saturated calomel reference electrode (SCE). Electrochemical testing was performed using a VMP 3Z potentiostat (Bio-Logic Instruments, USA).

The electrolytes used herein were unbuffered 0.1 M NaCl at pH 6, 0.1 M NaCl at pH 3 (pH adjusted using 0.1 g/L sodium acetate and 5.9 g/L acetic acid buffer), and 0.1 M NaCl at pH 11 (pH adjusted using 0.9 g/L sodium hydroxide and 2.1 g/L sodium hydrogen carbonate buffer). All electrolytes were quiescent natural aerated at 25 °C.

A galvanostatic-potentiostatic technique (as previously reported for electrochemical testing of pure Mg[14]) was used to qualitatively and quantitatively evaluate the anodically induced cathodic activation observed in the different metals. The electrochemical signal employed consisted of a 2-minute relaxation period prior to commencement of testing, after which the open circuit potential (OCP) value was measured. For each metal, a galvanostatic anodic current was applied in a stepwise manner from 0.025 to 20 mA/cm^2, with each polarisation having an 'on' period of 2 minutes. In between each galvanostatic polarisation signal, a 2 minute potentiostatic signal was applied at a fixed cathodic potential value (i.e. –2 V_{SCE}), to measure the corresponding cathodic current supported by the - previously anodically polarised - surface. The cathodic current measured at -2 V_{SCE} corresponds to anodically induced cathodic activation. The currents were measured after 1 second intervals during the potentiostatic step. In order to undertake a comprehensive analysis, two separate test methodologies were employed. The first methodology employed the abovementioned galvanostatic steps and potentiostatic interrogation of cathodic reaction rate at a fixed potential of -2 V_{SCE} (enabling a direct contrast for the HER rate of all metals at a fixed potential); the second methodology employed the abovementioned galvanostatic steps; however, with the potentiostatic applied potential being at a fixed cathodic overpotential with respect to OCP of each metal, namely at -0.5 V vs. the OCP. The latter test was considered

useful on the basis that all the metals tested had a unique OCP, and thus a direct comparison should include both comparison at a fixed potential, and also at a fixed cathodic overpotential with respect to the OCP. All experiments were repeated for each metal at least 5 times, to ensure both reproducibility and to provide a range of results (and hence reported results below include error bars representing standard deviations). Selected specimens were also imaged by an optical microscope after electrochemical testing. Scanning electron microscopy (SEM) was performed on selected samples using and FEI Quanta 3D-FEG.

3. Results and discussion

Electrochemical testing

The typical results collected from the custom galvanostatic-potentiostatic cycle testing for two metals, Sn and Mg, are present and shown in **Fig. 1.**

These metals were chosen as two examples in order to also show the accompanying raw data and the typical differences in electrochemical response observed. Electrochemical testing involved the application of the cyclic test protocols previously described, and in the case of the data in Figure 1, both examples (Sn and Mg) are cycled to the fixed cathodic potential of -2 V_{SCE} in 0.1 M NaCl at pH 6 (**Fig. 1**). What can be readily observed is that the cathodic current measured upon Sn is higher than that measured upon Mg, as the fixed potential of -2.0 V_{SCE} provides a much higher cathodic polarisation for Sn ($OCP_{Sn,\ pH6}$ = -0.7V_{SCE}) as opposed to Mg ($OCP_{Mg,\ pH6}$ = -1.65V_{SCE}). It is for this reason that additional testing, reported below, also employs comparisons of cathodic current at a fixed polarisation from OCP.

In order to assess the relative rate of the cathodic reaction during the potentio-static cathodic cycle, the cathodic current is taken at the end of the potentiostatic period (as denoted by an 'x' in Fig. 1). What can be observed is that the cathodic current densities following prior anodic polarisation, in spite of the anodic polarisation extending to attain exceptionally high currents (20 mA/cm^2) as measured for Sn, remained essentially constant (**Fig. 1a**). This suggests that Sn does not undergo cathodic activation after prior anodic polarisation. In contrast, for pure Mg, the kinetics of the cathodic reaction were found to increase after each anodic galvanostatic cycle (**Fig. 1b**), indicating that Mg indicates cathodic activation arising from prior dissolution. Due to the differing response of Sn and Mg, they were presented here in 0.1 M NaCl at pH 6 as two typical examples for which raw data is presented, however the remainder of the data presented, and its analysis are in abridged format.

The abridged results for Sn and Mg are presented for the results from the galvanostatic-potentiostatic cycling tests at pH 3, 6 and 11 – as seen in **Fig. 2a-b**. The data in **Figs. 2a-b** reports the cathodic current densities (measured at – 2 V_{SCE}) following the denoted prior anodic polarisation. From such a representation it is evident that Sn does not display cathodic activation (from cathodic analysis at -2 V_{SCE}) regardless of electrolyte pH. In contrast, the plot reveals a clear indication of cathodic activation for Mg in 0.1 M NaCl with pH 6 and 11, and to a lesser extent, cathodic activation in the electrolyte of pH 3 (**Fig. 2b**). Additionally, in near-neutral unbuffered solution (pH 6), the localised surface pH was expected to increase

during the experiments, due to the formation of hydroxyl ions induced by HER and relatively slow rates of metallic ions hydrolysis.

Analysis of cathodic activation for the various metals studied

Prior to the application of the galvanostatic-potentiostatic cycling, the OCP of the metals studied was measured for all the pH conditions tested. To provide a broader context to the results herein, the OCP values of the different metals studied herein following a 2-minute relaxation period are reported in **Fig. 3**.

The relative nobility of the different metals studied based on OCPs in near-neutral electrolyte (pH 6) 0.1 M NaCl was determined to have the following order, Ge > Pb > Sn > Sc > Al > Gd > Mg > La. Gd, Mg and La are considered to support HER as the primary cathodic reaction upon their surfaces as they both have very negative values of OCP (<< -1V_{SHE}). The other metals tested herein have a relatively more noble OCP and therefore are likely to favour ORR upon their surfaces as the primary cathodic reaction. In the case of where the cathodic reaction rates are kinetically assessed at the fixed potential of -2 V_{SCE}, all metals are probed (at that potential) for their ability to support the HER. In the case of where cathodic reaction rates are kinetically assessed at the fixed cathodic potential with respect to OCP - 0.5 V, the relative extent of HER supported will vary, however the point is to assess the degree of cathodic activation per se, as opposed to the absolute cathodic current. The influence of pH on the OCP values of Ge, Sc, Gd, La and Mg was not significant, however the OCP values of Pb, Sn, and Al, all decreased with an increase in pH.

As the core contribution of the present study, the abridged volume of data for cathodic currents measured during the respective potentiostatic signals after each galvanostatic step for all metals, in the three different electrolytes, are summarised in **Figs. 4-6**.

As mentioned, cathodic currents were measured at -2 V_{SCE} and -0.5 V vs. the OCP of the respective metal (**Fig. 4-6)**. In order to further assess the notion of cathodic activation a metric was created, whereby the ratio of increase in cathodic kinetics (as defined by Eq. 1 below) after each galvanostatic step, was also determined and compared for the different metals tested herein (as also shown in **Fig. 4-6**).

$$\text{Dynamic increase in cathodic kinetics} = \frac{i_x}{i_1} \qquad \text{(Eq. 1)}$$

Where i_x is measured cathodic current density during each potentiostatic cycle (following anodic exposure) and i_1 is the measured cathodic current density from the first cycle.

The results of electrochemical tests when measured at the two potentiostatic conditions, at -2 V_{SCE} and also -0.5 V_{SCE} vs the OCP, generally revealed a similar trend. However, there was an expected variation in the absolute cathodic current measured (which is itself a function of cathodic polarisation). The metals Sc, Gd, La and Mg revealed cathodic activation in 0.1 M NaCl with pH ranging 3-11 (**Fig. 4-6**). In contrast Sn, Pb and Ge do not reveal cathodic activation. Uniquely, and discussed further below in the general discussion, Al revealed cathodic activation only after prior anodic polarisation in acidic (0.1 M NaCl, pH 3) conditions.

The results indicate that the extent of cathodic activation for the metals Sc, Gd and La was lower in acidic conditions as compared to neutral and alkaline conditions. At pH 3 only a slight enhancement of cathodic was observed for the elements Sc, Gd and La (**Fig. 5**). A greater enhancement of HER kinetics was however observed for Sc, Gd and Mg in neutral and alkaline solutions (**Fig. 4-6**). The incremental increase in enhanced cathodic activity was proportional to increasing solution pH. For Mg, the increase in cathodic reaction kinetics was ~4.25 times of the initial (pre-anodic polarisation) value, following the galvanostatic cycling regime at pH 6. For pH 11 solution however, the increase in cathodic activity was ~6.4 times of the initial value. In contrast, the non-cathodic activation elements Ge, Sn, and Pb, indicated a relatively steady rate of cathodic kinetics after the galvanostatic-potentiostatic cycling for all pH conditions tested. This in its own right merits comment, as the galvanostatic dissolution will inherently alter the surface area (by roughening due to metal dissolution). However, in spite of this inherent surface area alteration, the subsequent overall cathodic kinetics were not significantly altered.

In regards to extending the concepts covered in the introduction and critically appraising the data collected herein, it is possible to make the following statement based on empirical results and for the metals studied herein that reveal cathodic activation. That is, the presence of cathodic activation occurred for metals that are known as ‘hydroxide formers’. In order to explore this somewhat further, the E-pH diagrams of the metals tested herein are presented. These diagrams, show the thermodynamically stable pH-potential domains for the different chemical species, formed in the metal-water system. The OCP values of the different metals in the pH range 3-11 are overlaid upon the E-pH diagram of the corresponding metal (**Fig. 7**

a-h)[38]. As well-known from the reported Pourbaix diagrams[38], the metals Sc, Gd, La and Mg have the higher tendency to form metal hydroxides as the pH of the solution becomes more alkaline (**Fig. 7 a-d**). These metals have a lower free enthalpy of formation for forming their corresponding hydroxides, than for forming their oxides[38]. The metals Sc, Gd, La and Mg could therefore readily form metal hydroxides. It is also of interest to note that for the case of Mg, it has recently been reported that the near surface pH can readily alkalise, whilst additionally, the ability to form a surface hydroxide can also occur at pH values much lower than those predicted by the Pourbaix diagram[39]. The work of Williams and co-workers revealed that Mg-hydroxide may possibly form at pH values in the neutral range, based on results from density functional theory modelled surface Pourbaix diagrams[39]. Conversely, Al, Sn, Pb and Ge do not readily form metal hydroxides, in the pH-potential domains corresponding to their measured OCP values (**Fig. 7 e-h**). In fact, for these metals, the metal oxide is more thermodynamically stable than the metal hydroxide[37]. Additionally, we also notice another salient feature among the metals that display cathodic activation. These metals all have very negative values of the standard reduction potential for the M/M^{n+} redox couple (where M is the metallic element and n is the chemical valency). The standard reduction potentials of the metals which display cathodic activation are as follows, -2.09 V_{SHE} for Sc, -2.38 V_{SHE} for La, -2.28 V_{SHE} for Gd and -1.98 V_{SHE} for Mg[40]. Therefore, another contribution to the cathodic activation may be the communality of a significant galvanic driving force for all these metals in terms of anodic dissolution coupled with the HER on the impurity metal phases.

Surface inspection

Whilst detailed surface analysis was not conducted in the present study, the surface morphologies of the different metals tested following the galvanostatic-potentiostatic cycle tests (assessed at the fixed potential of -2 V_{SCE}) in 0.1 M NaCl (pH 6) are shown in **Fig. 8**.

In the case of Mg, Sc, Gd, and La, the surface products formed upon the specimens reveal the characteristic dark appearance, as seen upon Mg and previously reported by several researchers[6, 7, 14, 20]. Such darkening of the metal surface after anodic polarisation is anticipated and considered to serve as primary cathodic sites for HER, on the basis of surface conditions concomitant with previous reports of cathodic activation of Mg[6, 19]. In contrast, comparatively 'whitish' or semi-opaque corrosion products were seen upon Al, Sn and Ge after the galvanostatic-potentiostatic cycle tests. The Pb surface however, also had a dark

appearance following the electrochemical testing, but this darkness did not appear to be similar to the aforementioned dissolution products of the metals displaying cathodic activation. This appearance may be due to the dark colour of Pb itself or due to the presence of finely divided metal colloids on the surface.

Following completion of the galvanostatic-potentiostatic cycle tests SEM was carried out upon several metals. The selected metals were all from testing in 0.1 M NaCl at pH 6, and represented two metals (Sc and Gd) which revealed cathodic activation, along with two metals (Sn and Ge) which did not reveal cathodic activation (**Fig. 9 a-d**). What can be determined from such images is that for the metals which indicate cathodic activation, both Sc and Gd form a dissolution product layer of metal hydroxides that could be seen upon their surfaces. Such a hydroxide layer is typically identified by the presence of 'mud cracks' in SEM images, whereby the mud cracks are a result of surface film dehydration (whereby the metal hydroxide layer is nominally a hydrated compound). Furthermore, the presence of only the pure metal and oxygen (noting that H cannot be detected by energy dispersive x-ray spectroscopy (EDXS)) were determined to be the only elements present from EDXS analysis (not presented herein). Based on the morphology observed, the relative thickness, and the presence of dehydration mud cracks, the surfaces seen in **Figs. 9a** and **9b** are believed to be metal hydroxides of Sc and Gd.

In contrast to Sc and Gd, the metals Sn and Ge presented with very different surface morphology after the galvanostatic-potentiostatic cycle tests. In the case of Sn, dissolution took the form of crystallographic dissolution, revealing dissolution led to surface roughening, and did not lead to the development of thick surface films. In the case of Ge, the dissolution observed was highly localised, and not associated with surface film development or thickening. Such dissolution morphologies seen from Sn and Ge are very distinct from the cathodically activating Sc and Gd.

General discussion

Several important findings can be drawn from the results of this body of work. Undoubtedly the work is both finite and preliminary in the context that only a selection of metals was studied, and analytical surface spectroscopy (to confirm the prevalence of metal hydroxides) was not carried out. None the less, the work is unique in its context, and several key discussion points arise. It was determined that the kinetics of the HER increases upon the surfaces of Sc, Gd, La and Mg, after prior anodic polarisation. These metals therefore

experience cathodic activation after anodic polarisation, and this is persistent in solutions of various pH, ranging from 3-11. Sn, Pb and Ge did not show cathodic activation in any of the three pH variants tested. Meanwhile, Al showed cathodic activation only in the acidic solution – which is interesting and unique, and in its own right will require further work to understand. The notion of NDE occurring upon Al is in fact, not new, having been carefully studied by Dražić and Popić[41] and more recently revisited by Curioni and co-workers[42]. A unique feature of cathodic activation revealed by Al herein, is that it only occurred in acidic conditions (where Al is prone to depassivation/pitting), and was manifest when the prior applied anodic dissolution rate was high. Whilst not the focus of present work, the notion of cathodic activation of Al, and the conditions where it occurs are worthy of an important comment. Acidic conditions are associated with a lack of film upon Al, wherein the reactive bare metal surface is exposed to the solution. This surface could therefore participate in direct reaction with water. In such an instance, the notion of having a 'reactive bare metal surface' could be inferred as the origin of cathodic activation (in the absence of further analysis). This concept of a 'reactive bare metal surface' is an important concept to hold – more generally – as future work, whilst the formation of hydroxides and the enrichment of noble metals are important factors that associated with cathodic activation, the contribution from other factors cannot be ruled out in a holistic framework. Focusing again on the work presented herein, it can be stated that a causal relationship was presented, we believe for the first time, whereby metals which form metal hydroxides (as judged from the Pourbaix diagrams) by direct chemical reactions with water - have a tendency to display cathodic activation. More recently, a density function theory (DFT) study performed by Yuwono et al.[43] suggested that hydroxyl group adsorption in aqueous solution, reduced the surface work function of Mg, which consequently contributed to the enhanced cathodic catalytic activity upon the surface of Mg. The DFT study was in qualitative agreement with the experimental works present herein, where all the "hydroxide forming" metals studied, including Mg, Sc, Gd and La, exhibited significant cathodic activation.

4. Conclusions

Pure metals including Mg Sc, Gd, La, Sn, Al, Pb and Ge were subject to galvanostatic-potentiostatic cycling in order assess their cathodic kinetics (namely the rate of the HER), after prior anodic polarisation at different current densities. Electrochemical tests were conducted in 0.1 M NaCl at three different pH values of 3, 6 and 11. The study was able to survey the prevalence of cathodic activation in the selected metals tested, allowing a causal relationship to be presented between the presence of cathodic activation and the tendency of tested metal to form a metal-hydroxide. This generality of the causal relationship cannot be wholly assessed from the work herein alone, and will require wider study, however based on the results herein, the following specific conclusions were drawn:

- The metals Sc, Gd, La and Mg demonstrated an increase in the kinetics of HER (cathodic activation) following prior anodic polarisation / dissolution in electrolytes of different pH (from 3 to 11). Furthermore, the HER kinetics were also found to increase, with increasing applied anodic current densities during the anodic polarisation step.
- The extent of cathodic activation observed for Sc, Gd, La and Mg was found to vary with the pH of the test electrolyte. The absolute rate of HER kinetics realised after prior anodic polarisation was higher upon these metals when tested at higher pH values (i.e. pH 11 when compared to pH 3).
- For the metals Sn, Pb and Ge the kinetics of the HER were not significantly altered after prior anodic polarisation. These metals can therefore be considered to not demonstrate cathodic activation.
- In the case of Al metal, Al showed cathodic activation only when the sample was cycled and held at -0.5 V vs OCP, after prior anodic polarisation in acidic solution.
- The electrochemical responses collected herein were analysed and contrasted with the expected equilibrium surfaces from thermodynamic data (viz. Pourbaix diagrams) for the selected metals tested. It was revealed that metals which could directly react with water to form metal hydroxides such as Mg, La, Gd and Sc, demonstrated higher tendencies to undergo cathodic activation. These metals also possess highly negative standard reduction potentials (in the vicinity of -2 V_{SCE} or below).
- The metals which show cathodic activation (Sc, Gd, La and Mg) seem to dissolve by producing a dark film which consumes the “intact” surface with time.

Acknowledgements

We acknowledge the use of facilities in the Monash Centre for Electron Microscopy. RLL is supported by a Monash Graduate Scholarship and Faculty of Engineering International Postgraduate Research Scholarship. JRS is supported by NSF DMR #0906663 and JRS and NB gratefully acknowledge support from the U.S. Army Research Laboratory (agreement number W911NF-14-2-0005) with project leader Dr. Joseph P. Labukas.

References:

1. W. Beetz, *Philosophical Magazine Series* 32, 216 (1866): p. 269-278.
2. G.S. Frankel, A. Samaniego, N. Birbilis, *Corrosion Science* 70, (2013): p. 104-111.
3. R. Glicksmann, *Journal of the Electrochemical Society* 106, (1959): p. 83.
4. A.D. King, N. Birbilis, J.R. Scully, *Electrochimica Acta* 121, (2014): p. 394-406.
5. J.L. Robinson, P.F. King, *Journal of the Electrochemical Society* 108, 1 (1961): p. 36-41.
6. G. Williams, N. Birbilis, H.N. McMurray, *Electrochemistry Communications* 36, (2013): p. 1-5.
7. S. Thomas, N.V. Medhekar, G.S. Frankel, N. Birbilis, *Current Opinion in Solid State and Materials Science* 19, 2 (2014): p. 85-94.
8. R.L. Liu, M.F. Hurley, A. Kvryan, G. Williams, J.R. Scully, N. Birbilis, *Scientific reports* 6, (2016): p. 28747.
9. S. Fajardo, C.F. Glover, G. Williams, G.S. Frankel, *Electrochimica Acta* 212, (2016): p. 510-521.
10. L. Rossrucker, K.J.J. Mayrhofer, G.S. Frankel, N. Birbilis, *Journal of the Electrochemical Society* 161, 3 (2014): p. C115-C119.
11. F.W. Richey, B.D. McCloskey, A.C. Luntz, *Journal of the Electrochemical Society* 163, 6 (2016): p. A958-A963.
12. L. Yin, X. Huang, H. Xu, Y. Zhang, J. Lam, J. Cheng, J.A. Rogers, *Advanced materials* 26, 23 (2014): p. 3879-3884.
13. M. Taheri, J.R. Kish, N. Birbilis, M. Danaie, E.A. McNally, J.R. McDermid, *Electrochimica Acta* 116, (2014): p. 396-403.
14. N. Birbilis, A.D. King, S. Thomas, G.S. Frankel, J.R. Scully, *Electrochimica Acta* 132, (2014): p. 277-283.
15. G. Williams, H. Neil McMurray, *Journal of the Electrochemical Society* 155, 7 (2008): p. C340.
16. M. Curioni, *Electrochimica Acta* 120, (2014): p. 284-292.
17. G. Williams, N. Birbilis, H.N. McMurray, *Faraday discussions* 180, 0 (2015): p. 313-330.
18. J.D. Hanawalt, C.E.Nelson, J.A.Peloubet, *Trans AIME*, 147 (1942).
19. S. Thomas, O. Gharbi, S.H. Salleh, P. Volovitch, K. Ogle, N. Birbilis, *Electrochimica Acta* 210, (2016): p. 271-284.
20. D. Lysne, S. Thomas, M.F. Hurley, N. Birbilis, *Journal of the Electrochemical Society* 162, 8 (2015): p. C396-C402.
21. T. Cain, S.B. Madden, N. Birbilis, J.R. Scully, *Journal of the Electrochemical Society* 162, 6 (2015): p. C228-C237.
22. N. Birbilis, T. Cain, J.S. Laird, X. Xia, J.R. Scully, A.E. Hughes, *ECS Electrochemistry Letters* 4, 10 (2015): p. C34-C37.
23. R.E. McNulty, J.D. Hanawalt, *Journal of the Electrochemical Society* 81, 1 (1942): p. 423-433.
24. G.L. Makar, J. Kruger, *Journal of the Electrochemical Society* 137, 2 (1990): p. 414-421.
25. D.A. Jones, *Principles and Prevention of Corrosion*, 2nd ed.(Upper Saddle River, NJ: Prentice Hall, 1996).
26. Z.P. Cano, J.R. McDermid, J.R. Kish, *Journal of The Electrochemical Society* 162, 14 (2015): p. C732-C740.
27. Z.P. Cano, M. Danaie, J.R. Kish, J.R. McDermid, G.A. Botton, G. Williams, *Corrosion* 71, 2 (2015): p. 146-159.
28. M.P. Brady, G. Rother, L.M. Anovitz, K.C. Littrell, K.A. Unocic, H.H. Elsentriecy, G.L. Song, J.K. Thomson, N.C. Gallego, B. Davis, *Journal of the Electrochemical Society* 162, 4 (2015): p. C140-C149.
29. K.D. Ralston, S. Thomas, G. Williams, N. Birbilis, *Applied Surface Science* 360, (2016): p. 342-348.
30. L. Rossrucker, A. Samaniego, J.P. Grote, A.M. Mingers, C.A. Laska, N. Birbilis, G.S. Frankel, K.J.J. Mayrhofer, *Journal of the Electrochemical Society* 162, 7 (2015): p. C333-C339.
31. S. Lebouil, A. Duboin, F. Monti, P. Tabeling, P. Volovitch, K. Ogle, *Electrochimica Acta* 124, (2014): p. 176-182.

32. S.H. Salleh, S. Thomas, J.A. Yuwono, K. Venkatesan, N. Birbilis, *Electrochimica Acta* 161, (2015): p. 144-152.
33. T. Cain, J.R. Scully, (2016).
34. S. Thomas, I.S. Cole, Y. Gonzalez-Garcia, M. Chen, M. Musameh, J.M.C. Mol, H. Terryn, N. Birbilis, *Journal of Applied Electrochemistry* 44, 6 (2014): p. 747-757.
35. M. Stratmann, H. Streckel, *Corrosion Science* 30, 6 (1990): p. 681-696.
36. M. Stratmann, H. Streckel, *Corrosion Science* 30, 6 (1990): p. 697-714.
37. A. Pishtshev, S.Z. Karazhanov, M. Klopov, *Solid State Communications* 193, (2014): p. 11-15.
38. M. Pourbaix, *Atlas of Electrochemical Equilibria in Aqueous Solutions*, 2nd English ed.(Houston, Tex.: National Association of Corrosion Engineers, 1974).
39. K.S. Williams, J.P. Labukas, V. Rodriguez-Santiago, J.W. Andzelm, *Corrosion* 71, 2 (2015): p. 209-223.
40. D.C. Harris, *Quantitative Chemical Analysis*, 6th ed.(New York; Basingstoke: W. H. Freeman; Palgrave Macmillan, 2002), p. AP20-AP27.
41. D.M. Dražić, J.P. Popić, *Journal of Applied Electrochemistry* 29, 1 (1999): p. 43-50.
42. M. Curioni, F. Scenini, *Electrochimica Acta* 180, (2015): p. 712-721.
43. J.A. Yuwono, N. Birbilis, K.S. Williams, N.V. Medhekar, *The Journal of Physical Chemistry C*, (2016).

(a)

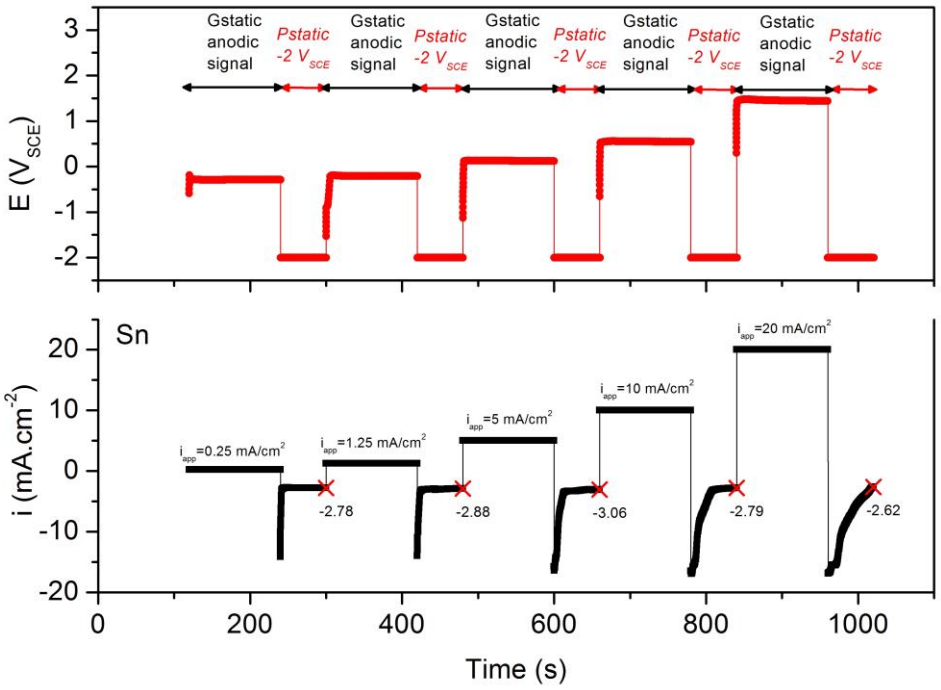

(b)

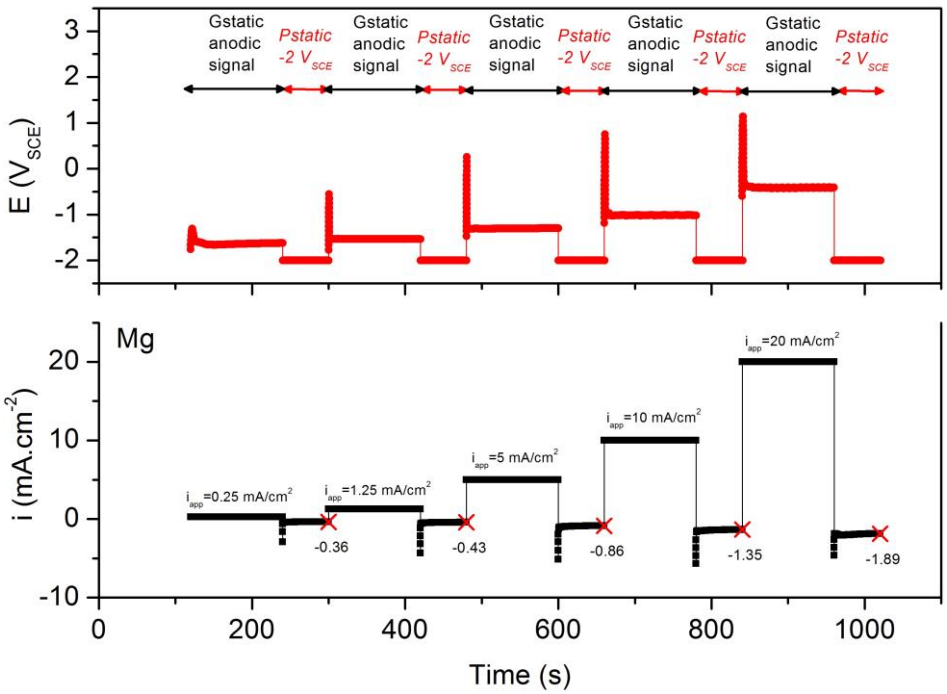

Figure 1. A representation of selected typical raw data collected via a galvanostatic-potentiostatic cycling test applied to: (a) Sn, and (b) Mg in 0.1 M NaCl (pH 6). The galvanostatic signal was applied in a stepwise manner (from 0.25 to 20 mA/cm^2) with 2 min duration. A 1 min duration potentiostatic signal at fixed potential of -2 V_{SCE} was applied between each galvanostatic signal and the corresponding cathodic current was measured (as marked "X" symbol on the curve) to determine the cathodic current after each galvanostatic step.

(a)

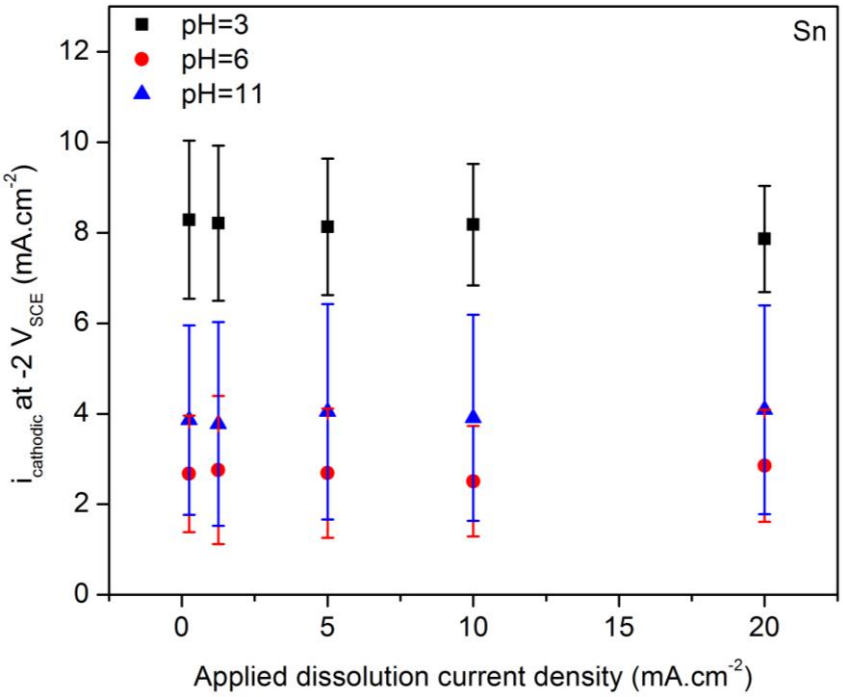

(b)

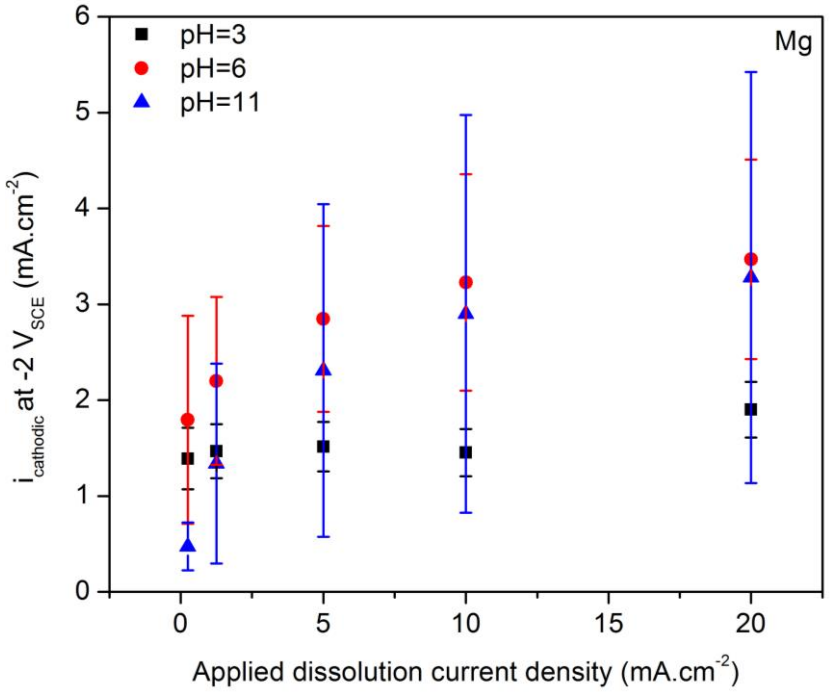

Figure 2. The measured cathodic current at -2V_{SCE} as determined following a 2 min galvanostatic anodic polarisation step for (a) Sn and (b) Mg. Average results reported for testing in 0.1M NaCl at pH 3, 6 and 11.

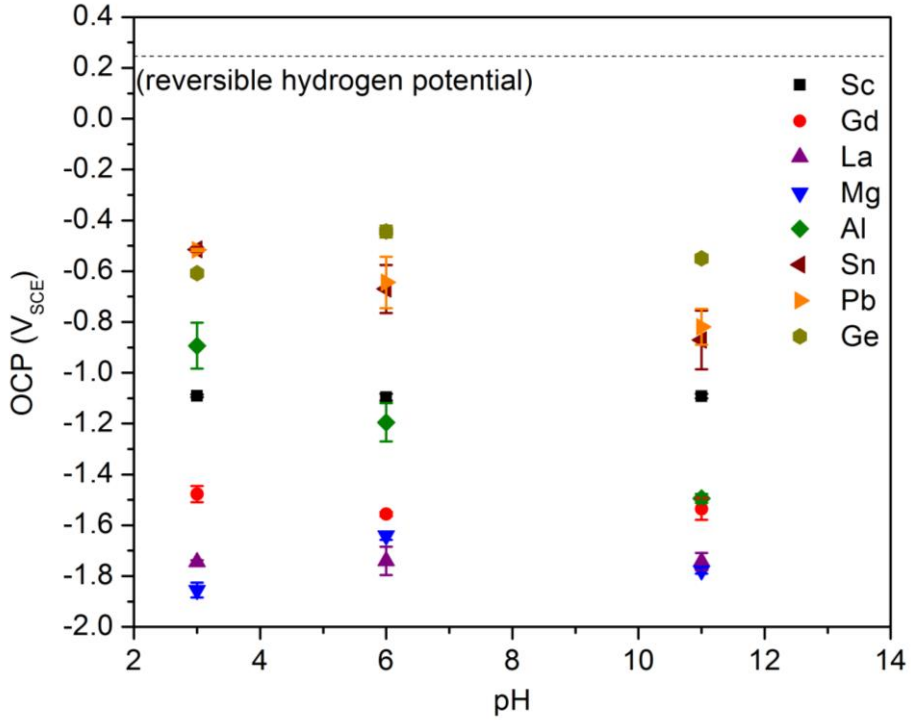

Figure 3. Open circuit potential (OCP) of the metals tested herein for pH 3, 6 and 11, after 2 minutes of exposure to 0.1 M NaCl solution.

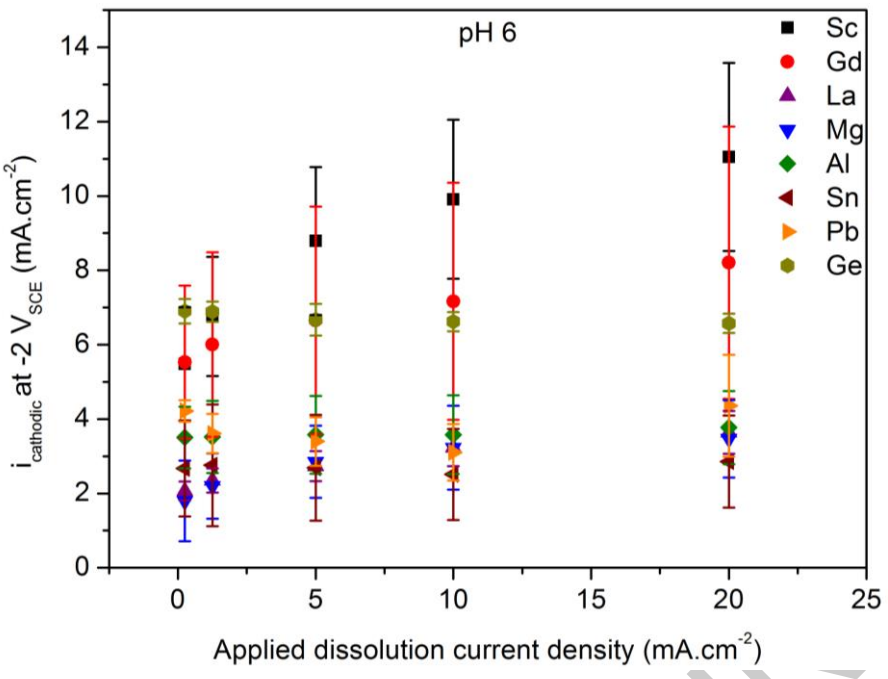
pH 6
Sc
Gd
La
Mg
Al
Sn
Pb
Ge
$i_{cathodic}$ at -2 V_{SCE} (mA.cm^{-2})
Applied dissolution current density (mA.cm^{-2})
0
2
4
6
8
10
12
14
0
5
10
15
20
25

(a)

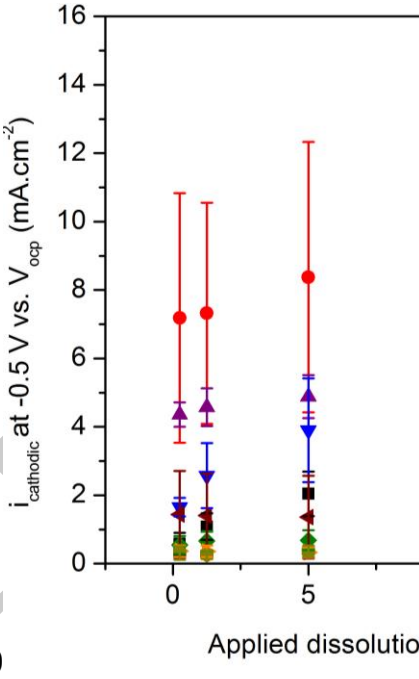
$i_{cathodic}$ at -0.5 V vs. V_{ocp} (mA.cm^{-2})
Applied dissolutio
0
2
4
6
8
10
12
14
16
0
5

(b)

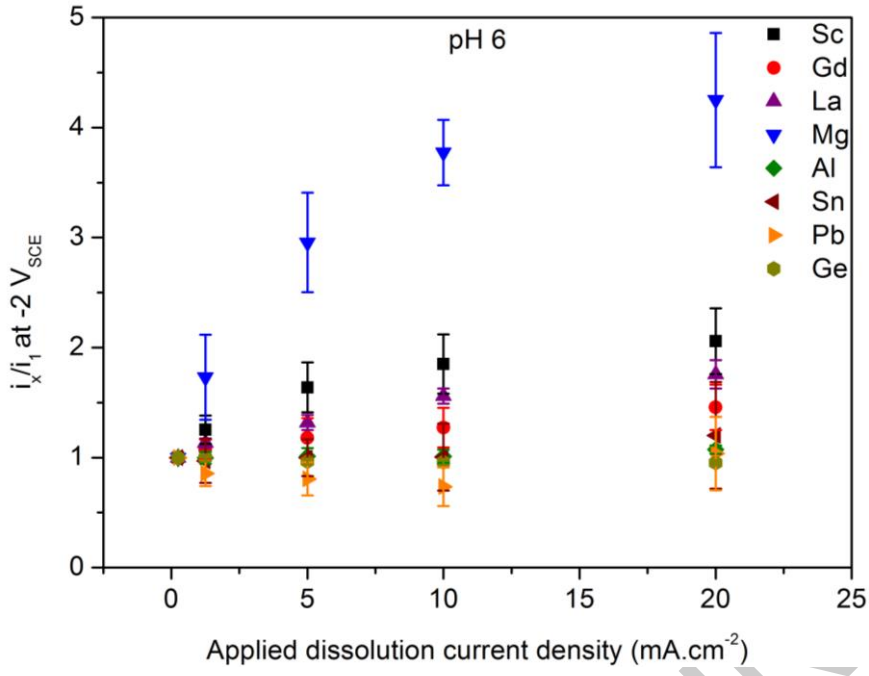

Figure 4. The summarised results from galvanostatic-potentiostatic testing for the various metals tested he current density ($i_{cathodic}$) in 0.1 M NaCl (pH 6); (a) measured at -2 V_{SCE} and (b) measured at -0.5V_{SCE} vs. OC metals measured at (c) -2 V_{SCE}, (d) -0.5V_{SCE} vs. OCP are also shown.

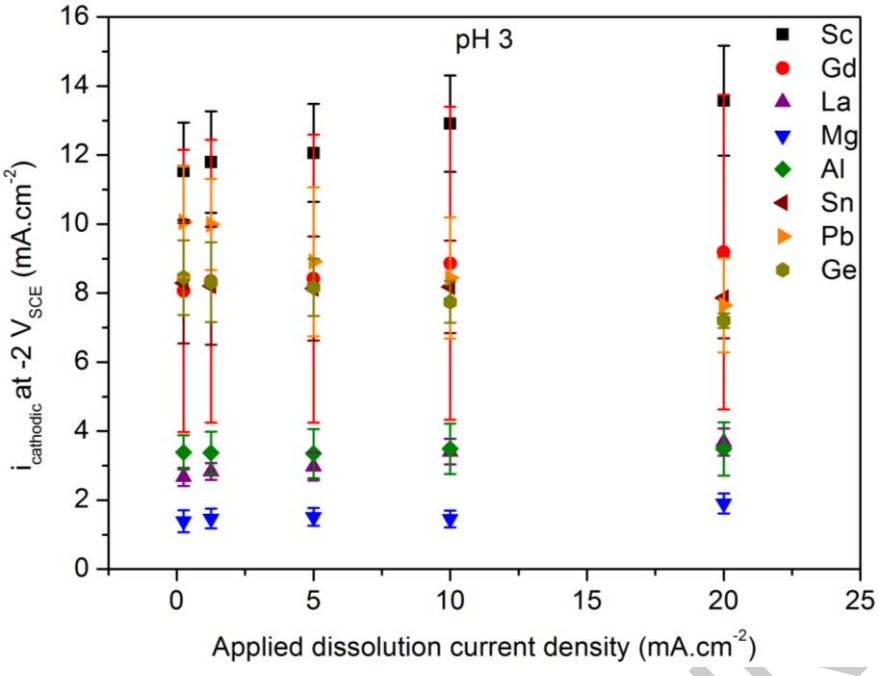
pH 3
Sc
Gd
La
Mg
Al
Sn
Pb
Ge
$i_{cathodic}$ at -2 V_{SCE} (mA.cm^{-2})
Applied dissolution current density (mA.cm^{-2})
0
2
4
6
8
10
12
14
16
0
5
10
15
20
25

(a)

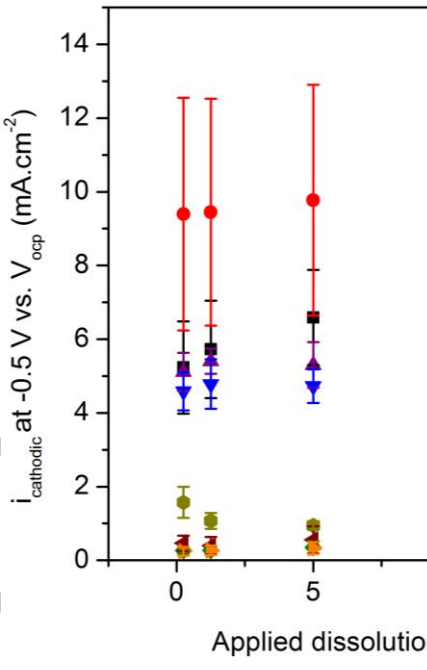
$i_{cathodic}$ at -0.5 V vs. V_{ocp} (mA.cm^{-2})
Applied dissolutio
0
2
4
6
8
10
12
14
0
5

(b)

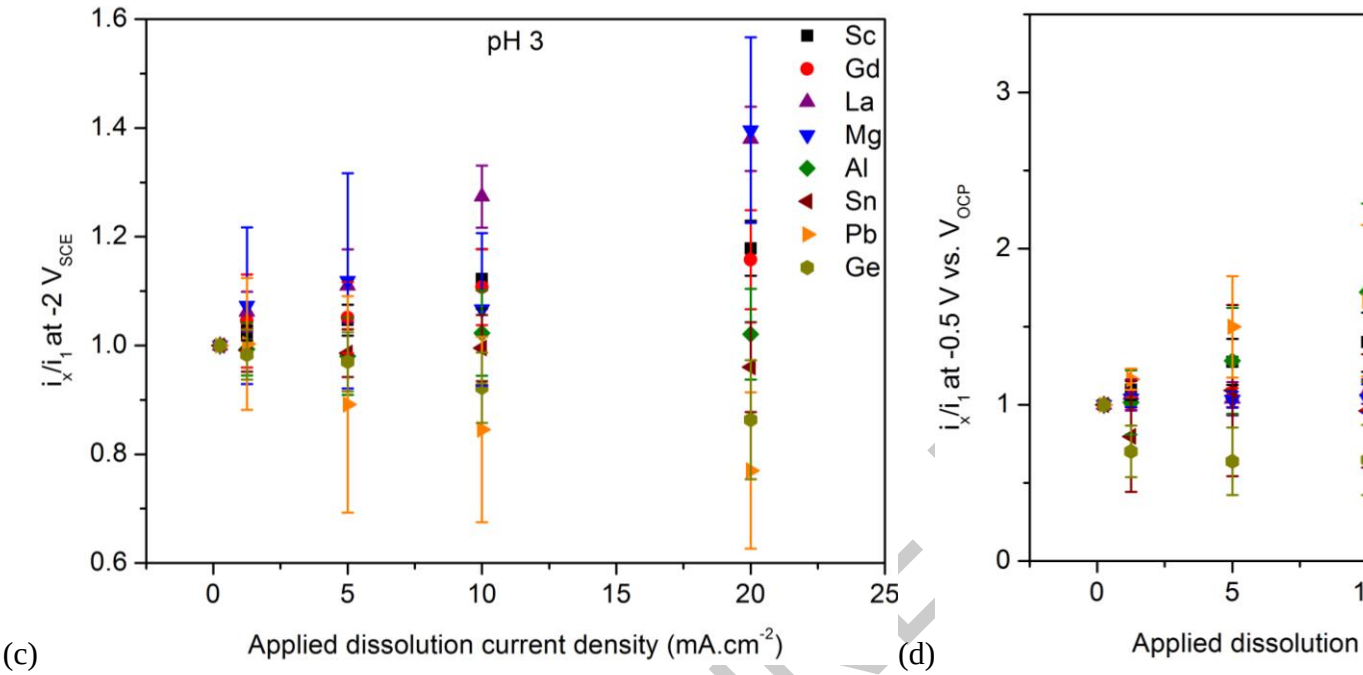

(c) (d)

Figure 5. The summarised results from galvanostatic-potentiostatic testing for the various metals tested he current density ($i_{cathodic}$) in 0.1 M NaCl (pH 3): (a) measured at -2 V_{SCE} and (b) measured at -0.5V_{SCE} vs. OC metals measured at (c) -2 V_{SCE}, (d) -0.5V_{SCE} vs. OCP are also shown.

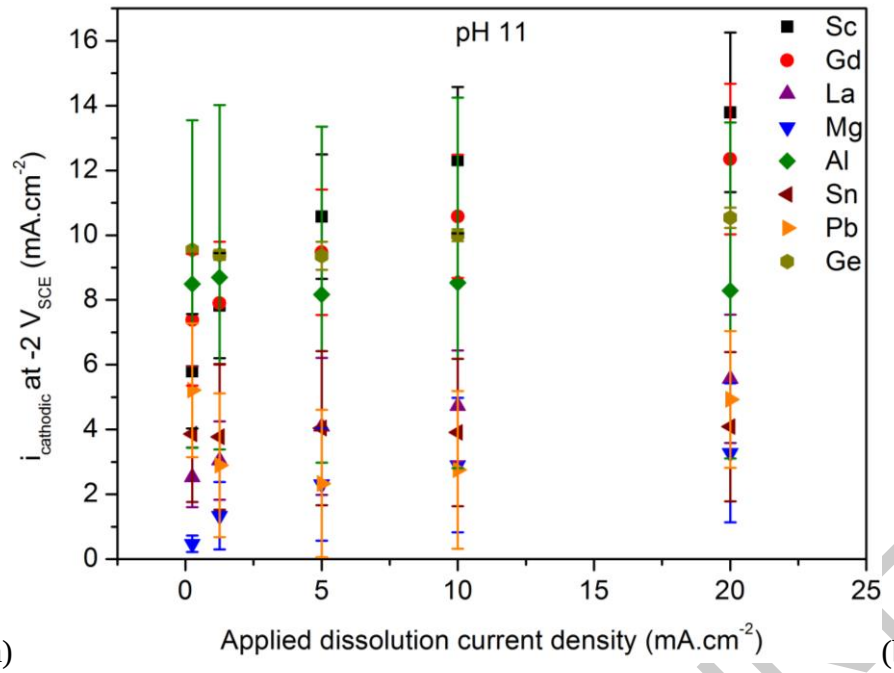
pH 11
Sc
Gd
La
Mg
Al
Sn
Pb
Ge
$i_{cathodic}$ at -2 V_{SCE} (mA.cm^{-2})
Applied dissolution current density (mA.cm^{-2})
0
2
4
6
8
10
12
14
16
0
5
10
15
20
25

(a)

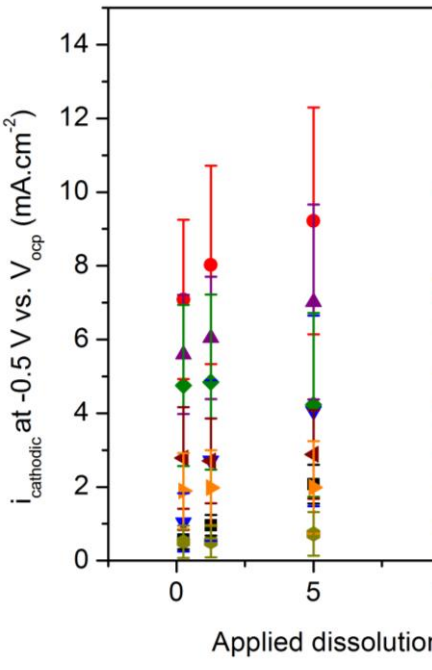
$i_{cathodic}$ at -0.5 V vs. V_{ocp} (mA.cm^{-2})
0
2
4
6
8
10
12
14
0
5

(b)

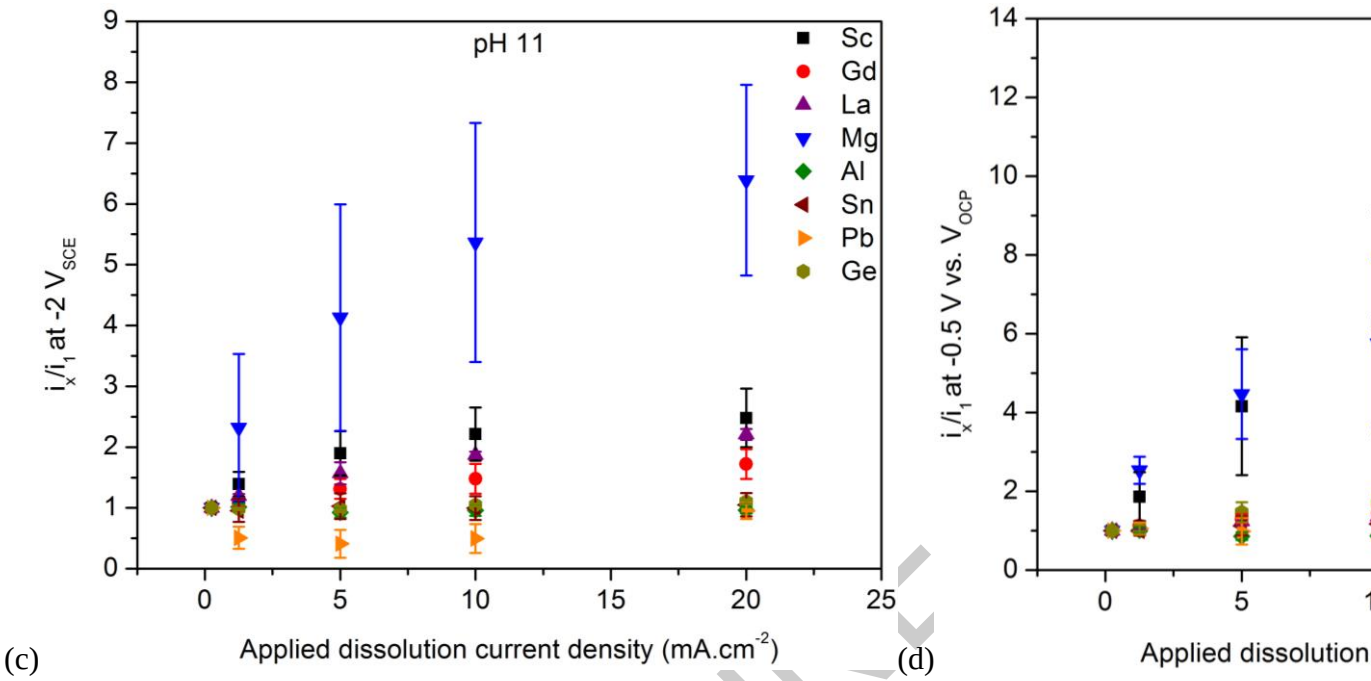

Figure 6. The summarised results from galvanostatic-potentiostatic testing for the various metals tested he current density ($i_{cathodic}$) in 0.1 M NaCl (pH 11): (a) measured at -2 V_{SCE} and (b) measured at -0.5V_{SCE} vs. O metals measured at (c) -2 V_{SCE}, (d) -0.5V_{SCE} vs. OCP are also shown.

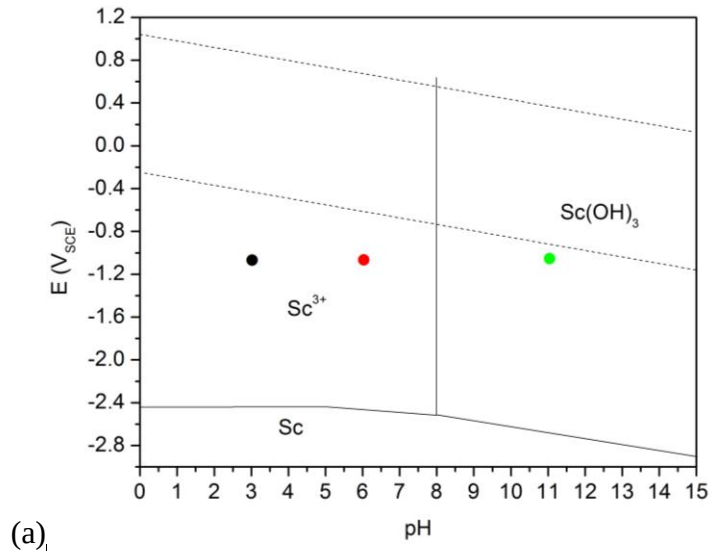
E (V_SCE)
pH
Sc(OH)3
Sc3+
Sc

(a)

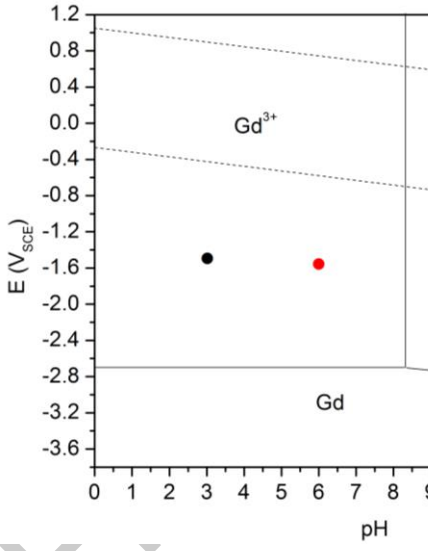
E (V_SCE)
pH
Gd3+
Gd

(b)

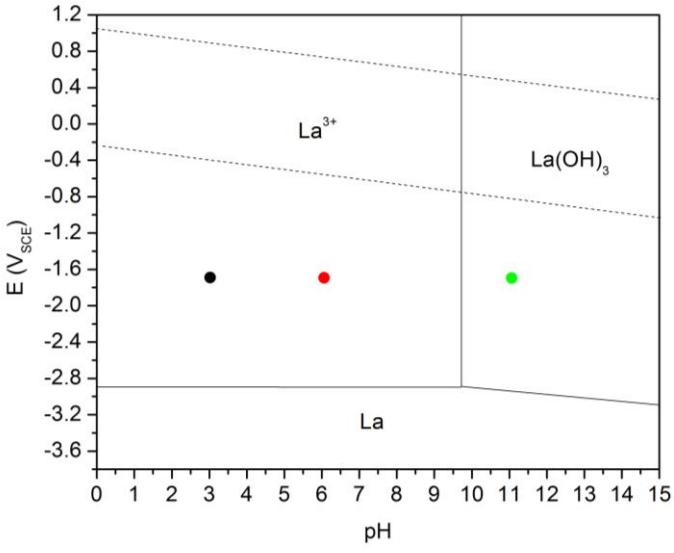
E (V_SCE)
pH
La3+
La(OH)3
La

(c)

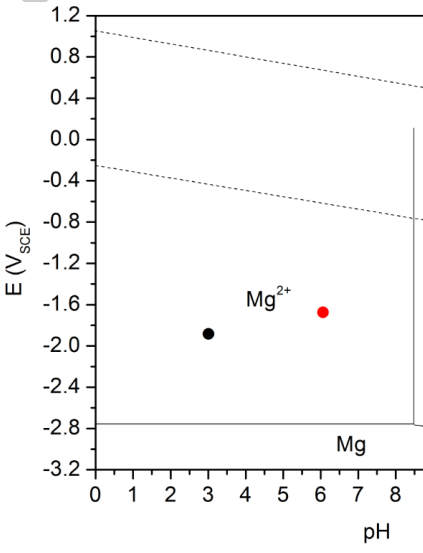
E (V_SCE)
pH
Mg2+
Mg

(d)

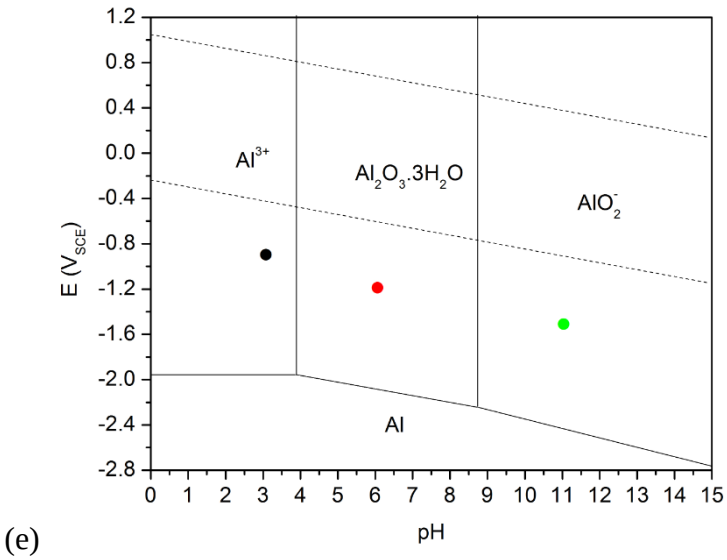

(e)

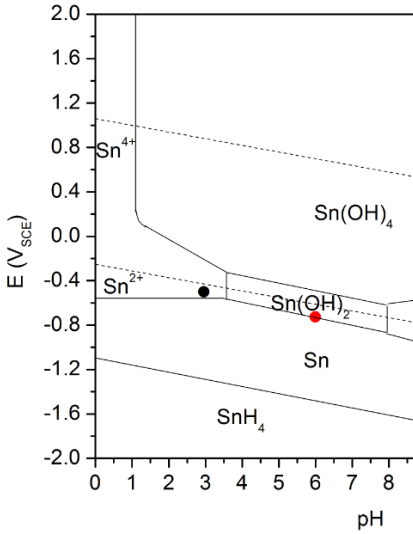

(f)

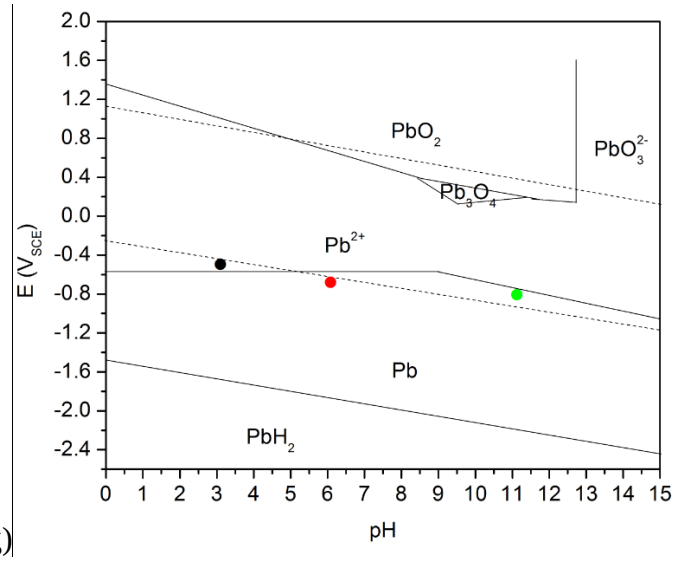

(g)

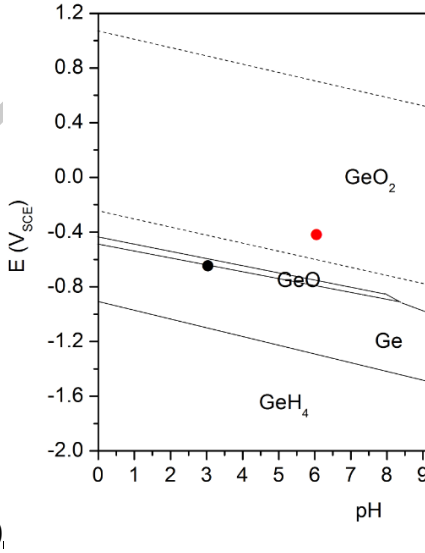

(h)

Figure 7. E-pH diagrams for: (a) Sc, (b) Gd, (c) La, (d) Mg, (e) Al, (f) Sn, (g) Pb and (h) Ge. The values of cor
also marked on respective E-pH diagram of respective elements38. The values of open circuit potential at pH 3,
respective E-pH diagram. All potentials on such diagrams are reported relative to the satura

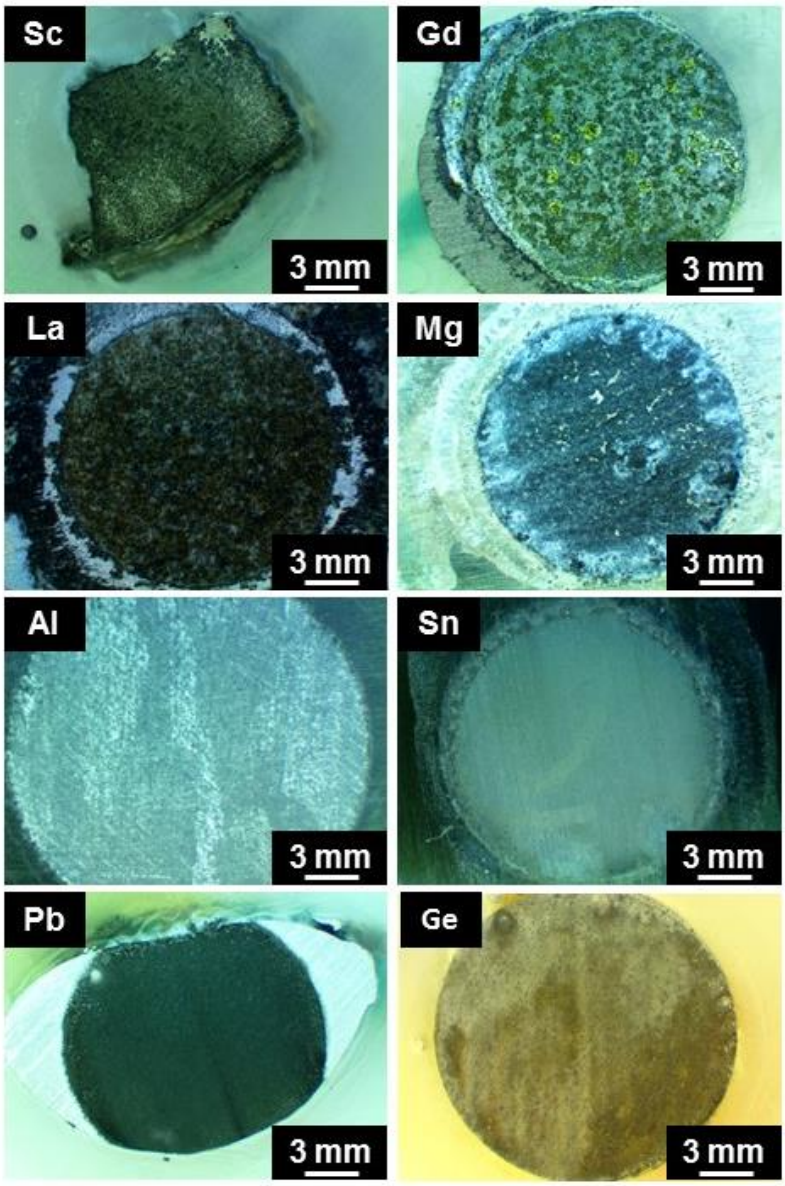

Figure 8. The surface morphologies of the different metals tested after the galvanostatic-potentiostatic cycle test (assessed at the fixed potential of -2 V_{SCE}) in 0.1 M NaCl (pH 6) for Sc, Gd, La, Mg, Al, Sn, Pb and Ge.

(a)

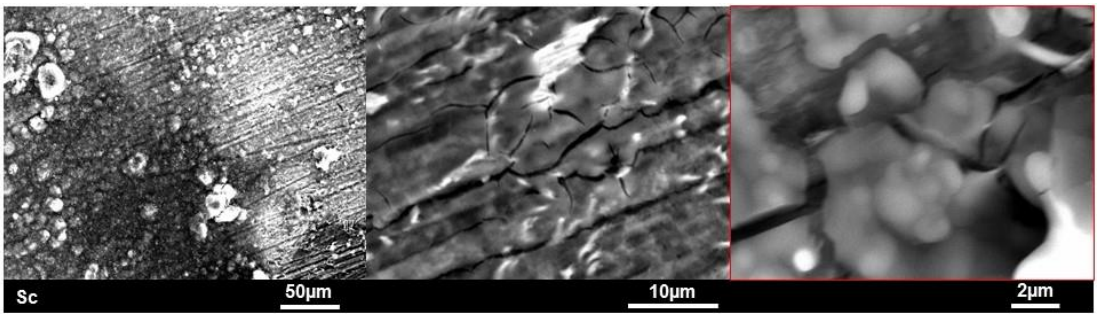

(b)

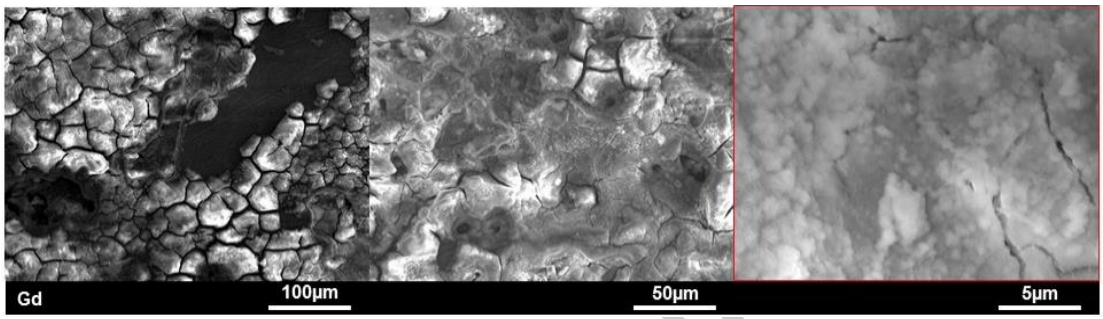

(c)

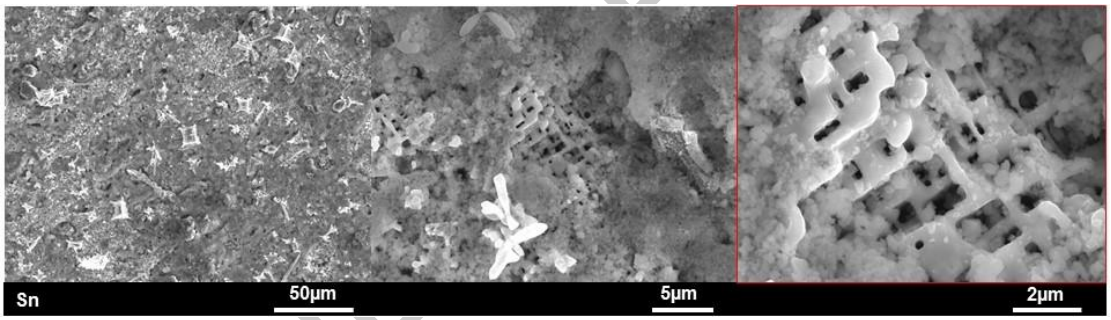

(d)

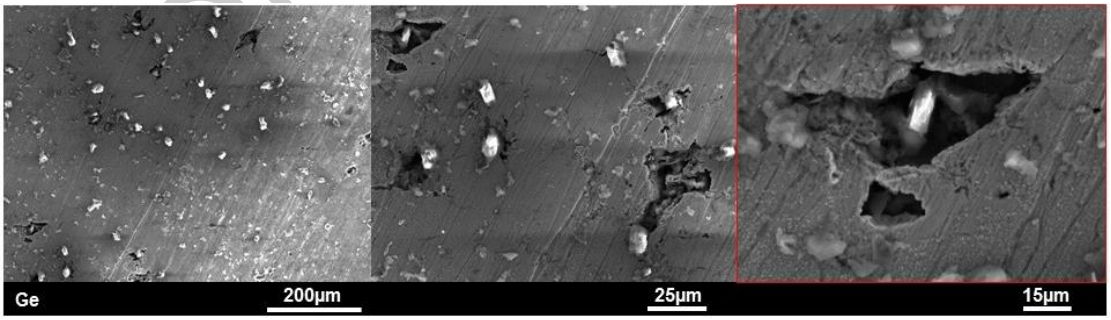

Figure 9. Scanning electron microscopy images of selected metals after the galvanostatic-potentiostatic cycle test in 0.1 M NaCl (pH=6) for: Sc (a), Gd (b), Sn (c), and Ge (d). Low (left), intermediate (middle) and high (right) magnification images presented.